

PROBE FOR TYPE IA SUPERNOVA PROGENITOR IN DECIHERTZ GRAVITATIONAL WAVE ASTRONOMY

TOMOYA KINUGAWA

Institute for Cosmic Ray Research, University of Tokyo, Kashiwa, Chiba 255-8582, Japan

HIROKI TAKEDA

Department of Physics, Kyoto University, Kyoto 606-8502, Japan and
Department of Physics, University of Tokyo, Bunkyo, Tokyo 113-0033, Japan

ATARU TANIKAWA

Department of Earth Science and Astronomy, College of Arts and Sciences, The University of Tokyo, 3-8-1 Komaba, Meguro-ku, Tokyo 153-8902, Japan

HIROYA YAMAGUCHI

Institute of Space and Astronautical Science, JAXA, 3-1-1 Yoshinodai, Sagami-hara, Kanagawa 229-8510, Japan and
Department of Physics, University of Tokyo, Bunkyo, Tokyo 113-0033, Japan

(Dated: September 15, 2022)
Draft version September 15, 2022

ABSTRACT

It is generally believed that Type Ia supernovae are thermonuclear explosions of carbon-oxygen white dwarfs (WDs). However, there is currently no consensus regarding the events leading to the explosion. A binary WD (WD-WD) merger is a possible progenitor of Type Ia supernovae. Space-based gravitational wave (GW) detectors with considerable sensitivity in the deci-Hz range such as the DECI-hertz Interferometer Gravitational wave Observatory (DECIGO) can observe WD-WD mergers directly. Therefore, access to the deci-Hz band of GWs would enable multi-messenger observations of Type Ia supernovae to determine their progenitor and explosion mechanism. In this paper, we consider the event rate of WD-WD mergers and minimum detection range to observe one WD-WD merger per year, using a nearby galaxy catalog and the relation between the Ia supernova and host galaxy. Furthermore, we calculate DECIGO's ability to localize WD-WD mergers and to determine the masses of binary mergers. We estimate that the deci-Hz GW observatory can detect GWs with amplitudes $h \sim 10^{-20} [\text{Hz}^{-1/2}]$ at 0.01-0.1 Hz, which is 1000 times higher than the detection limit of DECIGO. Assuming progenitors of Ia supernovae are merging WD-WD ($1M_{\odot} - 0.8M_{\odot}$), DECIGO is expected to detect 6600 WD-WD mergers within $z = 0.08$, and identify the host galaxy of such WD-WD mergers within $z \sim 0.065$ using GW detection alone.

1. INTRODUCTION

Advanced LIGO have detected gravitational waves (GWs) from compact binary mergers. These GWs have reveal the existence of massive stellar black holes, and the origin of the r-process elements and short gamma-ray burst (Abbott et al. 2016a,b, 2017). We are at the dawn of GW astronomy. Ground GW detectors such as advanced LIGO, advanced VIRGO, and KAGRA cover 10–10,000 Hz. LISA is designed to detect milli Hz GWs and will launch during the 2030s (Amaro-Seoane et al. 2017, 2022). The design sensitivity of LISA is $h \sim 10^{-20} [\text{Hz}^{-1/2}]$ at 0.01 Hz. DECIGO and B-DECIGO, a test version of DECIGO, fill the gap between the ground GW detectors and LISA (Seto et al. 2001; Nakamura et al. 2016). The main target of DECIGO is the stochastic background GW from the early universe. Design sensitivity of DECIGO and B-DECIGO are $h \sim 10^{-23}$ – $10^{-24} [\text{Hz}^{-1/2}]$, and $h \sim 10^{-22}$ – $10^{-23} [\text{Hz}^{-1/2}]$ at 0.1–10

Hz, respectively. These sensitivities are very useful to detect high redshift binary black hole mergers and check the origin of massive stellar black holes (e.g. Kinugawa et al. 2014; Kinugawa et al. 2016; Belczynski et al. 2016; Nakamura et al. 2016; Kinugawa, Nakamura, & Nakano 2020; Tanikawa et al. 2022). Furthermore, the GW from a white dwarf-white dwarf (WD-WD) merger is also $\sim 0.01 - 0.1$ Hz (Dan et al. 2011; Mandel et al. 2018). Thus, WD-WD mergers will become interesting science targets of DECIGO (Seto et al. 2001; Mandel et al. 2018) and other 0.1 Hz GW detectors such as B-DECIGO (Nakamura et al. 2016), TianGO (Kuns et al. 2019), DO(Arca Sedda et al. 2019) and AMIGO (Ni et al. 2019).

WD-WD mergers are one of the most promising candidates of Ia supernova progenitors. Although Ia supernovae have considerable significance as distance indicators in cosmology, many fundamental aspects of their evolution and explosion are still under debate (see a recent review by Ruiter 2020). It is widely accepted that the Ia supernova progenitor system is a carbon-oxygen (C-O) WD in an interacting binary star. However, the nature of the companion star and the WD

kinugawa@icrr.u-tokyo.ac.jp
takeda@tap.scphys.kyoto-u.ac.jp
tanikawa@ea.c.u-tokyo.ac.jp
yamaguchi@astro.isas.jaxa.jp

mass are unclear. The companion star can be a non-degenerate star (main sequence, giant-like or stripped-helium-burning star), or another WD, also known as single degenerate (SD) and double degenerate (DD) scenarios, respectively. The WD mass can be near the Chandrasekhar limit, $\sim 1.4M_{\odot}$, (Chandrasekhar-mass explosion), or below the limit (sub-Chandrasekhar-mass explosion). For the SD scenario with the Chandrasekhar-mass explosion, the WD approaches the Chandrasekhar limit via mass transfer from its non-degenerate companion star (e.g. Whelan, & Iben 1973; Nomoto 1982a; Hachisu et al. 1996). For the SD scenario with the sub-Chandrasekhar-mass explosion, a C-O WD accretes helium-rich materials from its companion helium star, and initiates double detonation explosion in which helium detonation on the WD surface leads to detonation of carbon in the WD core (Nomoto 1982b; Woosley et al. 1986; Livne 1990).

The DD scenario with Chandrasekhar-mass explosion can occur tidal disruption of the lighter WD followed by thermal mass accretion onto the heavier WD (e.g. Webbink 1984; Iben, & Tutukov 1984). For the DD scenario with sub-Chandrasekhar-mass explosion, three things can occur. First, a dynamical merger of two C-O WDs initiates carbon detonation directly, referred to as a carbon-ignited violent merger (e.g. Pakmor et al. 2010; Sato et al. 2015). Second, it can result in another explosion mode known as spiral instability (Kashyap et al. 2015, 2017). Lastly, a dynamical mass accretion onto the heavier C-O WD from lighter helium-rich WD triggers double detonation explosion, referred to as a helium-ignited violent merger or a dynamically-driven double-degenerate double-detonation (D6) (e.g. Guillochon et al. 2010; Fink et al. 2010; Woosley, & Kasen 2011; Pakmor et al. 2013; Shen, & Bildsten 2014). In the DD scenario with Chandrasekhar explosion, Ia supernovae may occur ~ 100 yr or more after the WD-WD mergers due to slow mass accretion. Conversely, in the DD scenario with sub-Chandrasekhar-mass explosion, Ia supernovae occur promptly around the time of WD-WD merger. Thus, if any sub-Chandrasekhar-mass explosion models do occur, WD-WD mergers emit GW and electromagnetic (EM) signals at the same time, it can be a promising target of multi-messenger astronomy. This can be applied to identifying progenitors of subclasses of Ia supernovae.

In this paper, we consider the event rate of WD-WD mergers and minimum detection range to observe one WD-WD merger per year, using the nearby galaxy catalog and the relation between the Ia supernova and host galaxy (§2). Furthermore, we investigate the observational performance of DECIGO for WD-WDs by the parameter estimation of the inspiral GWs from WD-WD mergers. Mainly, we evaluate the detection rate and the ability of these detectors to localize WD-WD mergers and to determine the masses of binary mergers (§3, 4, and 5). Throughout this paper, we use CGS units except for §3.

2. EVENT RATE OF WD-WD MERGERS

In order to estimate the WD-WD merger rate, we assume that all the Ia supernova progenitors are WD-WD mergers. Note that this assumption ignores the possibility of the SD case. However, Maoz et al. (2018) shows that the expected WD-WD merger rate in the Milky Way is 4.5–7 times more than its specific Ia supernova rate.

Thus, the WD-WD merger rate from our assumption might be smaller than the actual value.

The Ia supernova rate at $z \sim 0$ is

$$(0.301 \pm 0.062) \times 10^{-4} \text{ SN yr}^{-1} \text{ Mpc}^{-3}, \quad (1)$$

determined from the Lick Observatory Supernova Search (LOSS) (Li et al. 2011). We use this value as the fiducial rate of WD-WD mergers to estimate the detection rate in this paper. However, this rate is the averaged volumetric rate of Ia supernova. The relation between WD-WD mergers and Ia supernovae can be confirmed by the early detection of the first GW from a WD-WD merger and its electromagnetic (EM) counterpart. This is similar to the GW170817 where the relation between binary neutron star mergers and short GRBs+kilonovae was revealed (Abbott et al. 2017). We need to determine the minimal detection volume to detect a WD-WD merger per year in the nearby galaxies. There are many studies on the rate-size relation of Ia supernova host galaxies (e.g. Sullivan et al. 2006; Totani et al. 2008; Li et al. 2011; Childress et al. 2014; Graur et al. 2015) and these results indicate the relation between Ia supernova rate and the stellar mass of the galaxies. In order to estimate the event rate of Ia supernova near our galaxy, we consider the rate-size relation of Ia supernova host galaxy (Li et al. 2011) and the catalog of nearby galaxies within 11 Mpc (Karachentsev et al. 2013). The rate-size relation is

$$\text{SNuM} = \text{SNuM}(M_0) \times \left(\frac{M_*}{10^{10}M_{\odot}} \right)^{\text{RSS}}, \quad (2)$$

where SNuM, $\text{SNuM}(M_0)$, M_* , and RSS are the Ia supernova rate per century per $10^{10}M_{\odot}$, the normalization value, the stellar mass of the galaxy, and the power law index, respectively. Li et al. (2011) obtained -0.513 ± 0.316 , -0.503 ± 0.158 , -0.637 ± 0.199 , -0.555 ± 0.171 , -0.443 ± 0.241 , -0.329 ± 0.201 , and -0.435 ± 0.195 as RSSs for E, S0, Sa, Sb, Sbc, Sc, and Scd galaxies, respectively. The combined significance with $\text{RSS} = -0.5$ and $\text{SNuM}(M_0) = 0.25$ for E, S0, Sa, Sb, Sbc, Sc, and Scd galaxies is -7.4σ (Li et al. 2011). Thus, we adopt -0.50 and 0.25 as RSS and $\text{SNuM}(M_0)$ in our rate calculations, respectively.

We use the galaxy catalog of Karachentsev et al. (2013) in order to get the stellar mass of nearby galaxies. In this catalog, there are data on 1209 galaxies within 11 Mpc and 951 galaxies' masses or lower mass limits. Figure 1 shows the stellar mass distribution of nearby galaxies. In the case of galaxies whose masses are $\lesssim 10^5 M_{\odot}$, we use lower mass limits of galaxies as galaxy stellar masses.

We calculate the Ia supernova rate for each nearby galaxy using Eq.2 and stellar masses of nearby galaxies in this catalog data, and then take the sum of the Ia supernova rate in nearby galaxies within 11 Mpc. The summation of the Ia supernova rate in nearby galaxies is

$$0.85 \text{ yr}^{-1}. \quad (3)$$

This rate shows that approximately one Ia supernova will occur about once a year in nearby galaxies. If the detection range of GW detector on ~ 0.01 – 0.1 Hz band is more than 11 Mpc, the combination with the EM observation of supernova and the GW observation can be used to de-

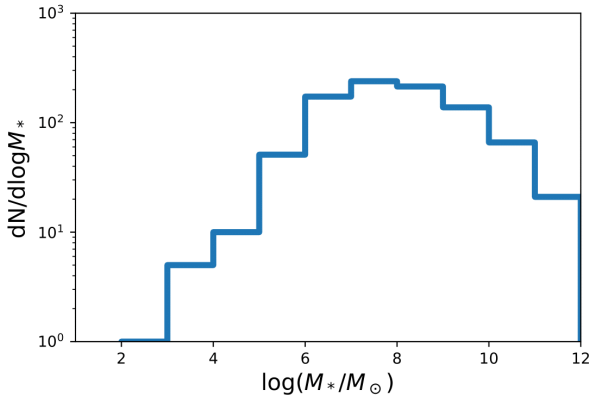


FIG. 1.— Stellar mass distribution of nearby galaxies within 11 Mpc.

termine whether Ia supernova progenitors are WD-WD mergers or not.

3. GRAVITATIONAL WAVEFORM FOR INSPIRALING BINARY WHITE DWARF

In this section, we use $c = G = 1$. In general relativity, the detector signal of a GW from an inspiraling binary system in time domain can be written as (Berti et al. 2005; Maggiore 2007),

$$h(t) \simeq \frac{2m_1 m_2}{r_s(t) d_L} \mathcal{A}(t) \cos\left(\int^t f_{\text{gw}}(t') dt' + \phi_p(t) + \phi_D(t)\right), \quad (4)$$

where m_1, m_2 are the masses of binary stars, $r_s(t)$ is the orbital relative distance, d_L is the luminosity distance to the binary system, f_{gw} is the frequency of the GW, and $\phi_D(t)$ is the Doppler phase. $\mathcal{A}(t)$ and $\phi_p(t)$ are defined by,

$$\mathcal{A}(t) := \sqrt{(1 + \cos^2 \iota)^2 F^+(t)^2 + 4 \cos^2 \iota F^\times(t)^2}, \quad (5)$$

$$\phi_p(t) := \arctan\left(\frac{2 \cos \iota F^\times(t)}{(1 + \cos^2 \iota) F^+(t)}\right). \quad (6)$$

where ι is the inclination angle of the binary system. Here, $F^+(t)$ is the antenna pattern functions for the plus polarization mode, and $F^\times(t)$ is that for the cross mode (Nishizawa et al. 2009).

As $(2m_1 m_2)/(r_s(t) d_L)$, $\mathcal{A}(t)$, $\phi_p(t)$, $\phi_D(t)$ vary in time slowly compared to $\int f_{\text{gw}}(t') dt'$, we can calculate the Fourier component $\tilde{h}(f)$ of the detector signal $h(t)$ by the stationary phase approximation (Maggiore 2007; Berti et al. 2005; Cutler 1998; Arun 2006; Takeda et al. 2019),

$$\tilde{h}(f) = \mathcal{A} f^{-7/6} e^{i\Psi(f)} \mathcal{G}_T(t(f)). \quad (7)$$

with the GW amplitude \mathcal{A} and the phase $\Psi(f)$. The geometrical factor for tensor modes \mathcal{G}_T is defined by

$$\mathcal{G}_T(t) := \frac{5}{4} \mathcal{A}(t) e^{i(\phi_p(t) + \phi_D(t))}. \quad (8)$$

$t(f)$ gives the relation between the time to coalescence and the frequency of the GW before merger (Maggiore 2007; Damour et al. 2001, 2002), which is defined by the

condition $f = f_{\text{gw}}(t(f))$,

$$t(f) := t_c - \frac{5}{256} \mathcal{M}^{-5/3} (\pi f)^{-8/3}, \quad (9)$$

where $\mathcal{M} := (m_1 m_2)^{3/5} (m_1 + m_2)^{-1/5}$ is the chirp mass and t_c is the coalescence time.

We adopt the inspiral waveform up to Newtonian order in amplitude \mathcal{A} and 2.5 post-Newtonian (PN) order in phase $\Psi(f)$ (Santamaría et al. 2010; Khan et al. 2016),

$$\mathcal{A} f^{-7/6} = \frac{1}{\sqrt{30} \pi^{2/3} d_L} \mathcal{M}^{5/6} f^{-7/6}, \quad (10)$$

and

$$\Psi(f) = 2\pi f t_c - \phi_c - \frac{\pi}{4} + \frac{3}{128} (\pi \mathcal{M} f)^{-5/3} \sum_{i=0}^5 \phi_i (\pi \mathcal{M} f)^{i/3}. \quad (11)$$

where ϕ_c is the phase at the coalescence time and ϕ_i are PN coefficients. The amplitude is kept up to the Newtonian order because of the consistency with the order in Eq. (9). The binary eccentricity is not considered for simplicity because WD-WDs are expected to have circular orbits due to tidal interactions (Willems et al. 2007; Ruiter et al. 2010). It has been reported that the deformations due to filling the Roche lobe or the existence accretion disk induce typical difference at the level of one percent or less for semi-detached WD-WDs with respect to the average strain amplitude (van den Broek et al. 2012). For the WD-WDs whose rotations are synchronized with the orbital motion, it has been reported that finite size effects and certain universal relation are helpful to identify the individual masses of binary WDs (Wolz et al. 2021). Effects of mass transferring and the tidal effect just before mergers are studied by Kremer et al. (2017) and McNeill et al. (2020), respectively. However, the chirp effect is larger in the decihertz band because WD-WDs can be observed until just before the merger. Therefore, we concentrate on the mass and position information that can be extracted from the inspiral chirp signal alone, and ignore these effects of the WDs for the sake of generality.

4. PARAMETER ESTIMATION

In order to investigate the possibility of identifying the properties of the WD-WDs as a progenitor of Ia supernova in decihertz GW astronomy, we conducted parameter estimation by Fisher analysis (Finn 1992; Cutler, & Flanagan 1994). A Fisher information matrix gives the Cramer–Rao bound of the system parameter. In other words, a Fisher information matrix tells us how precisely we can determine the model parameters by observations under strong signal and Gaussian noise assumptions. The Fisher information matrix Γ is calculated by

$$\Gamma_{ij} := 4\text{Re} \int_{f_{\min}}^{f_{\max}} df \sum_I \frac{1}{S_{n,I}(f)} \frac{\partial \tilde{h}_I^*(f)}{\partial \lambda^i} \frac{\partial \tilde{h}_I(f)}{\partial \lambda^j}, \quad (12)$$

where $S_{n,I}(f)$ is the I-th detector noise power spectrum and λ^i is the i-th binary parameter. The inverse of the Fisher information matrix gives the root mean square

error of a parameter $\Delta\lambda^i$, calculated by

$$(\Delta\lambda^i)_{\text{rms}} := \sqrt{\langle \Delta\lambda^i \Delta\lambda^i \rangle} = \sqrt{(\Gamma^{-1})^{ii}}, \quad (13)$$

where $\Delta\lambda^i$ is the measurement error of λ^i and $\langle \cdot \rangle$ denotes ensemble average. Then, the sky localization error is defined by

$$\Delta\Omega_s := 2\pi |\sin\theta_s| \sqrt{\langle (\Delta\theta_s)^2 \rangle \langle (\Delta\phi_s)^2 \rangle - \langle \Delta\theta_s \Delta\phi_s \rangle^2}. \quad (14)$$

Hereafter, we simply refer to $(\Delta\lambda_i)_{\text{rms}}$ as $\Delta\lambda_i$, and call it the estimation error of λ_i .

we have 11 model parameters in GR

$$(\log \mathcal{M}, \log \eta, t_c, \phi_c, \log d_L, \chi_s, \chi_a, \theta_s, \phi_s, \cos \iota, \psi_p), \quad (15)$$

where $\log \eta, \chi_s, \chi_a$ are the logarithm of the symmetric mass ratio $\eta := m_1 m_2 / (m_1 + m_2)^2$, the symmetric and the antisymmetric spin parameter, respectively. The fiducial values of $t_c, \phi_c, \chi_s, \chi_a$ are set to be zero. We impose the priors on the parameters having domain of definition; $\log \eta, \phi_c$, angular parameters $(\theta_s, \phi_s, \cos \iota, \psi_p)$, and spin parameters (χ_s, χ_a) .

We set the upper cutoff frequency to the frequency at the coalescence time. Here, we roughly give the frequency at which the distance between the WDs is equal to the sum of the WD radius

$$f_{\text{max}} \simeq \frac{1}{\pi} \sqrt{\frac{GM_{\text{tot}}}{(R_1 + R_2)^3}}, \quad (16)$$

from Kepler's 3rd law. The mass-radius relation for WDs is given by the equilibrium condition for the gravitational pressure and electron pressure (Koester & Chanmugam 1990). For calculation of the upper cutoff frequency, we adopt the following mass-radius relation

$$R_* \sim 0.011 \left(\frac{M_*}{M_\odot} \right)^{-1/3} R_\odot, \quad (17)$$

based on the fitting of the observational data given by Magano et al. (2017). Once the upper cutoff frequency is determined, the lower cutoff frequency is obtained by the integration time or the observational time using Eq. (9). Figure 2 shows the inspiral GW strains from equal-mass WD-WDs having three different masses together with the spectral strain sensitivities of the decihertz GW telescopes. The plotted detector sensitivities are the root of the power spectral densities of their design sensitivities. The GW strains are plotted from an equivalent source amplitude of $2f^{1/2} |\tilde{h}(f)|$ (Moore et al. 2015). The circle points denote the upper cutoff frequency, the diamond points correspond to 10 years before coalescence and the triangle points correspond to 3 years before coalescence, which are calculated from the time of merger and Eq. (9). Compared to the GWs from compact binary mergers such as black holes and neutron stars observed at present by the ground-based detectors, the GWs from WD-WDs are almost monochromatic. However, we observe the slight frequency sweep effect in the decihertz band compared to that in LISA band.

We evaluated the estimation errors of the WD-WD parameters by Fisher analysis with DECIGO as the representative of decihertz gravitational wave detectors. We assume that DECIGO is composed of three interferometers sharing the arms and has its design sensitivity. We

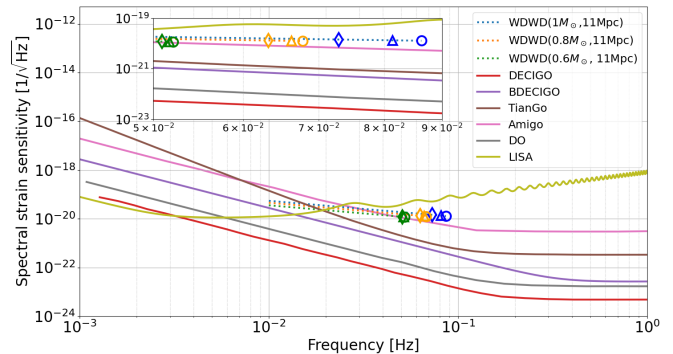


FIG. 2.— Spectral strain sensitivities of the decihertz GW detectors and the equivalents for the source amplitudes of the inspiral GWs from equal-mass WD-WDs with different masses at 11 Mpc. The upper cutoff frequency is given by the frequency at the coalescence from Eq. (16). The diamonds, triangles, and circle points correspond to 10 years, 3 years before merger, and the upper cutoff frequency, respectively.

also assume that its orbit is heliocentric orbit. The low-frequency approximation can be applied in all following calculations because the transfer frequency of the detector is $f_* := c/(2\pi L) \sim 48$ Hz corresponding to the arm length of $L = 1000$ km. Thereby, we ignore the transfer function in the antenna pattern functions (Romano & Cornish 2017). Unless otherwise noted, we conduct parameter estimation for the 100 binary systems whose distance is fixed to 11 Mpc, within which about one type Ia SN event is expected per year from Eq. (3), to estimate the typical but conservative values of the expected errors. We mainly show the median values of the estimated errors for such multiple sources when the angular parameters $(\cos\theta_s, \phi_s, \cos\iota, \psi_p)$ are randomly distributed.

5. RESULTS

5.1. Full period observation

First, we consider full observations during the 3 yr operation period. Figures. 3 and 4 show the fractional errors for the primary and the secondary WD component mass estimated by the Fisher analysis, respectively. The errors are estimated for 100 sources whose angular parameters are random for each mass combination by varying the component mass from $0.4M_\odot$ to $1.3M_\odot$ in $0.1M_\odot$ intervals, and the median value are shown in the color maps. The minimum median value of SNR is 9.59 for the $0.4M_\odot - 0.4M_\odot$ WD binaries and the maximum median value is 1240 for the $1.3M_\odot - 1.3M_\odot$ WD binaries. The results show that the mass ratio can be measured, and then the WD component mass can be identified in most of the $m_1 - m_2$ parameter space. The errors of the secondary WDs are almost the same, slightly smaller than those of the primary WDs. As the chirp mass is very well determined from the phase of the waveform, the error of the component mass is determined by the error of the mass ratio. If the mass of the primary WD is fixed, as the mass of the secondary WD decreases, the signal moves to a lower frequency band and the chirp effect decreases. As a result, the correlation among the chirp mass \mathcal{M} , the mass ratio η , the coalescence time t_c , and the right ascension ϕ_s increases, and the error of the mass ratio tends to increase. Nevertheless, for the WD-WDs containing a WD with the mass heavier than $0.8M_\odot$, the masses were found to be determined with less

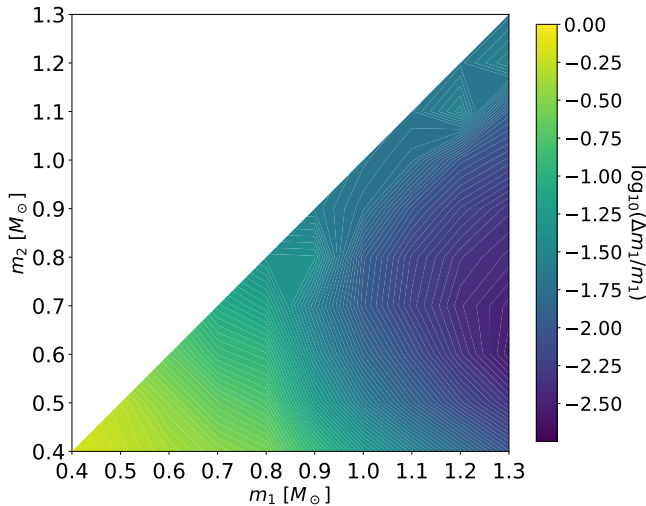


FIG. 3.— Median vales of the logarithms of the fractional estimation errors of the primary WD component mass $\log_{10}(\Delta m_1/m_1)$ for $m_1 - m_2$ WD-WDs at 11 Mpc. One Ia supernova event is expected per year within the distance from Eq. (3). The full observations during the 3 yr operation period are assumed.

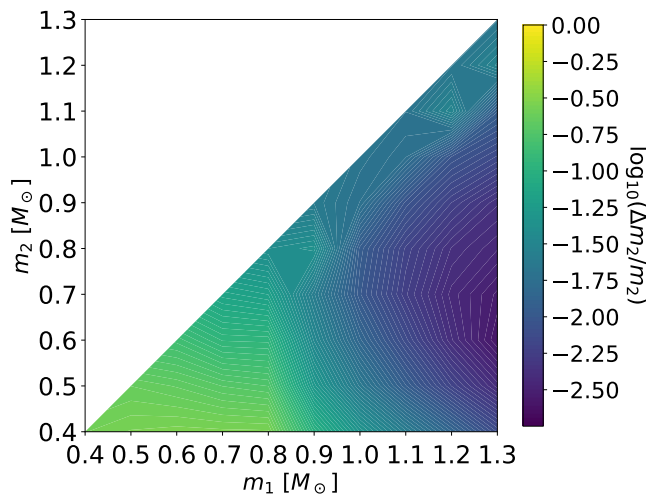


FIG. 4.— Similar to Figure 3 but for the secondary WD component mass.

than $\sim 10\%$ precision even from the chirp effect alone. We found the best fractional error of $\sim 0.3\%$ for masses $1.3M_\odot - 0.6M_\odot$.

Figure 5 shows the median values of the sky localization errors. It indicate that the more massive the mass, the smaller the error. The WD-WDs can be localized with the precision less than $\sim 5 \text{ deg}^2$ even for masses less than $0.8M_\odot$. The same trend as shown in Figure 5 was observed for d_L . We found that the luminosity distance can be determined with the precision less than 26%. Therefore, the WD-WDs can be localized with the 3D localization volume less than $\Delta V = d_L^3 \Delta \log d_L \Delta \Omega_s \sim 0.5 \text{ Mpc}^3$. In particular, for the WD-WDs containing a WD with the mass heavier than $0.8M_\odot$, we can determine the masses with the precision less than $\sim 10\%$, and the position with the 3D localization volume less than $\sim 1 \times 10^{-3} \text{ Mpc}^3$.

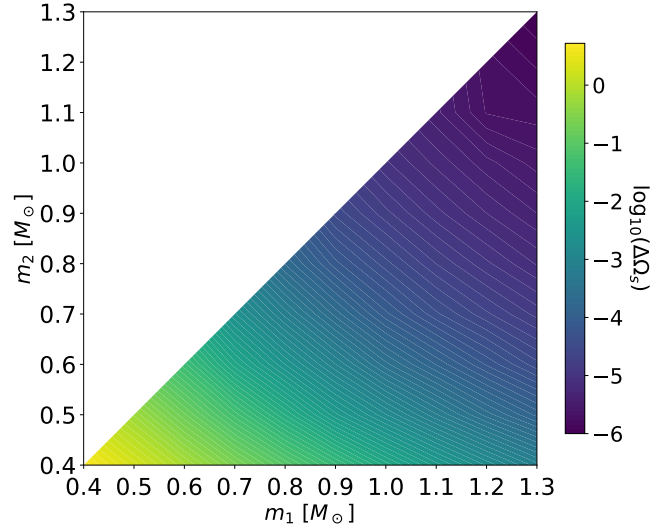


FIG. 5.— Median vales of the logarithms of the sky localization errors $\log_{10}(\Delta \Omega_s)$ for $m_1 - m_2$ WD-WDs at 11 Mpc. The full observations during the 3 yr operation period are assumed.

5.2. For multi-messenger observation

Next, we analyze how the determination precision changes with the different observation time for multi-messenger observations. As one example, we consider the $1M_\odot - 0.8M_\odot$ WD-WD case at 11 Mpc. We change the upper cutoff frequency before coalescence and calculate the parameter estimation errors for 100 WD-WDs whose angular parameters are random, whereas the lower cutoff frequency is fixed to 3 years before coalescence. Figure 6 shows the dependence of the median value of the estimation errors on the observational time. The GWs emitted from WD-WDs are regarded as almost monochromatic waves. The SNR increases as $\text{SNR}^2 \sim h_{\text{amp}} T / S_n(f)$. Thus, the errors such as Δm_1 and Δd_L seem to improve in proportion to $T^{-1/2}$, but in comparison, the actual errors are worse in the short observation period. This is owing to the fact that the chirp effect becomes smaller for shorter observation periods, and the correlations among the mass ratio and other parameters mentioned above becomes larger, resulting in stronger parameter degeneracy. If we measure for at least two year, from three years to one year before the coalescence, we can determine in advance the masses of the WDs with the precision less than 10% and its position with the 3D localization volume of 10^{-5} Mpc^3 .

Deci-Hz space-based detectors such as DECIGO are expected to observe WD-WDs at larger distances than LISA. To determine the typical decision precision for such distant WDs, we perform parameter estimation for WD-WDs fixed at a distance that gives the detection limit such that the SNR is approximately 8. Considering the $1M_\odot - 0.8M_\odot$ WD-WD case again, we fix the redshift $z = 0.08$ such that the median value of the SNR is approximately 8. Table 1 shows the median values of the parameter estimation errors for the logarithms of the component masses, the luminosity distance, the sky localization, and the 3D localization volume.

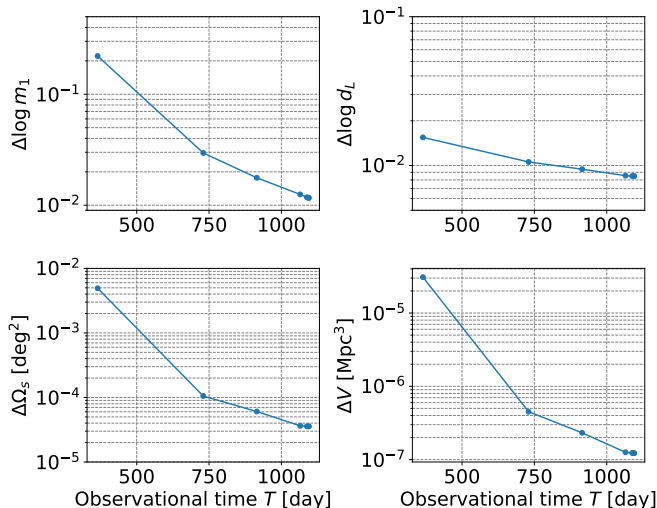


FIG. 6.— Estimation errors vs. observational time for $1.0M_{\odot} - 0.8M_{\odot}$ WD-WDs at 11 Mpc. The dots correspond to 2 years, 1 year, 6 months, 1 month, 1 week and 1 day before coalescence. The lower cutoff frequency is fixed to 3 years before the coalescence.

TABLE 1
MEDIANS OF THE PARAMETER ESTIMATION ERRORS FOR $1.0M_{\odot} - 0.8M_{\odot}$ WD-WDs FIXED AT $z = 0.08$ SO THAT THE MEDIAN VALUE OF THE SNR IS NEARLY EQUAL TO 8.

parameter	WD-WD($1M_{\odot}-0.8M_{\odot}$, $z=0.08$)
SNR	8.21
$\Delta \ln m_1$	1.84×10^{-1}
$\Delta \ln m_2$	1.54×10^{-1}
$\Delta \ln d_L$	3.00×10^{-1}
$\Delta \Omega_s [\text{deg}^2]$	6.66×10^{-2}
$\Delta V [\text{Mpc}^3]$	3.18×10^2

6. DISCUSSION & CONCLUSIONS

If the detection range of the deci-Hz detector is $D_L \sim 11$ Mpc, we may observe one WD-WD merger event per year. We need $h < 10^{-20} [\text{Hz}^{-1/2}]$ as the detection sensitivity around 0.1 Hz. In Figure 2, the AMIGO's sensitivity is same as this value; hence, the SNR may be small $\sim 1-2$. Conversely, the sensitivities of TianGO and B-DECIGO are both $\sim 3 \times 10^{-22} [\text{Hz}^{-1/2}]$, and DO's sensitivity is $\sim 5 \times 10^{-23} [\text{Hz}^{-1/2}]$. Thus, TianGO, B-DECIGO, and DO are sufficiently sensitive to detect a WD-WD merger whose SNR is more than 8.

For example, in the case of $1M_{\odot} - 0.8M_{\odot}$ WD-WD mergers, the median value of SNR is approximately equal to 8 when $z = 0.08 \sim 375$ Mpc. The detectable volume can be estimated as $2.2 \times 10^8 \text{ Mpc}^3$. Using Eq. (1), it is expected that approximately 6600 Ia supernovae would occur per year during the observational period within the range, assuming that all Ia supernovae are caused by $1M_{\odot} - 0.8M_{\odot}$ WD-WD mergers.

Furthermore, DECIGO can detect many inspirals of WD-WDs more than 3 years before their mergers at the 0.01–0.1 Hz range. Thus, we can investigate the mass and separation distribution of the WD-WDs and the relation between them and their host galaxies. Note that the detection rate estimate strongly depends on the masses

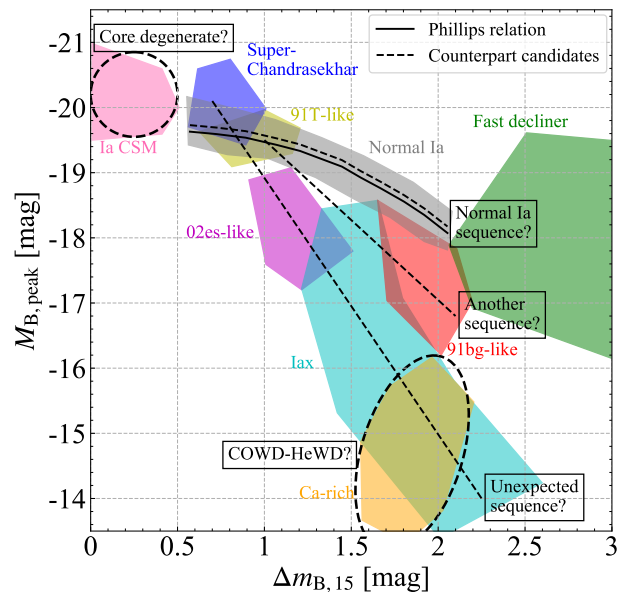


FIG. 7.— Peak magnitudes and decline rates in B band for normal Ia supernovae and subclasses of Ia supernovae, which is reproduced from figure 1 in Taubenberger (2017). The solid black curve shows the Phillips relation. The dashed black curves indicate counterpart candidates of WD-WD mergers supposed in the main text.

of WDs, as the GW frequency is proportional to the total mass of WD-WD (Eqs. 16 and 17).

The 3D localization volume of DECIGO $d_L^3 \Delta \ln d_L \Delta \Omega_s$ for $1M_{\odot} - 0.8M_{\odot}$ WD-WD mergers at $z = 0.08$ is 318 Mpc^3 . Conversely, the 3D localization volume WD-WD merger within $d_L \sim 11$ Mpc is $\sim 10^{-7} \text{ Mpc}^3$ (Figure 6). DECIGO provides a more useful and easier way to determine the host galaxy and its location compared to the host galaxy identification by LIGO observation. This value is proportional to d_L^6 due to $\Delta \ln d_L \propto d_L$ and $\Delta \Omega_s \propto d_L^2$. Thus, the 3D localization volume for $1M_{\odot} - 0.8M_{\odot}$ WD-WD mergers within $d_L \sim 300$ Mpc ($z = 0.065$) is $\sim 100 \text{ Mpc}^3$. The Milky Way-like galaxy density is one galaxy per 100 Mpc^3 (Kopparapu et al. 2008); hence, we can identify host galaxies for many WD-WD mergers using the GW detection only. It is useful and much easier to do follow-up observations and to identify the EM counterpart than the case of LIGO observation.

Multi-messenger (GW and EM) observations, will enable us to put unprecedented constraints on WD-WD merger outcomes and possibly Ia progenitors. First, we can confirm if WD-WD mergers cause prompt explosions and accompany bright astronomical transients as summarized in Figure 7. Then, if WD-WD mergers result in any transients, we can attribute to some types of thermonuclear transients. It is given that WD thermonuclear explosions are involved in various types of transients: normal Ia supernovae, subclasses of Ia supernovae (e.g. type Ia supernovae associated with circum-stellar matter (CSM), Super-Chandrasekhar Ia supernovae, SN 1991T-like, SN 1991bg-like, SN 2002es-like, and Iax supernovae), and Ca-rich transients (see review by Jha et al. 2019).

Owing to the high-quality mass estimate by GW observations (see Figures 3 and 4), we can assess the importance of WD masses. For example, let us assume that normal Ia supernovae results from WD-WD mergers; they will change their peak magnitudes and decline rates along with the Phillips relation (Phillips 1993) with changing WD masses. Then, we can attribute the physical background of the Phillips relation to WD masses (see “Normal Ia sequence” in Figure 7). By means of numerical simulations of WD explosions, Ruiter et al. (2013) indicated that the peak magnitudes depend on exploding WD masses, and Shen et al. (2018a) showed that the peak magnitudes and decline rates depend on exploding WD masses partly along with the Phillips relation. Conversely, GW observations will provide information of WD masses independently of such numerical simulations, and can be combined with EM observational results of the peak magnitudes and decline rates.

We further give three possibilities as examples. First, exploding WD masses may be responsible for the appearance of transients: normal Ia or subclasses of Ia supernovae (see “another sequence” in Figure 7). The violent merger model, one of the WD explosion models that may represent events after WD-WD mergers, is suggested to cause SN 1991-bg-like for primary WD masses with $\sim 0.9M_{\odot}$ (Pakmor et al. 2010), and normal Ia supernovae for primary WD masses with $\sim 1.1M_{\odot}$ (Pakmor et al. 2012). Second, the difference between exploding WD masses may yield an “unexpected sequence” (see Figure 7), ranging over Super-Chandrasekhar, 91T-like, 02es-like, and Iax supernovae. We should note that some of them may have *SD progenitors*, but not DD progenitors. Some super-Chandrasekhar Ia supernovae indicate massive CSM like SN 2012dn (Yamanaka et al. 2016). Iax supernovae can have bright companion stars like SN 2012Z (McCully et al. 2014). This is why we call it “unexpected” sequence. Third, a WD-WD merger, one of which has a small mass ($\lesssim 0.5M_{\odot}$), can generate a Ca-rich transient (Perets et al. 2010) as seen in “COWD-HeWD” in Figure 7. Note that a $\lesssim 0.5M_{\odot}$ WD is thought as a helium (He) WD.

The direct measurement of WD masses will also facilitate the determination of the combustion process of WDs, and emission process of Ia supernova ejecta. As for the combustion process, the peak magnitudes can be converted into radioactive nuclear masses, ^{56}Ni masses (Ruiter et al. 2013; Shen et al. 2018a). Thus, we can assess if carbon detonation, a promising combustion process in sub-Chandrasekhar mass WDs, can yield EM-observed ^{56}Ni masses from GW-observed WD masses. As for the emission process, the decline rates can be related to the opacity of supernova ejecta, WD masses (Hoeflich et al. 1996; Nugent et al. 1997; Maeda et al. 2003; Kasen & Woosley 2009). We can also verify if EM-observed decline rates are consistent with GW-observed WD masses.

Even if a WD-WD merger is a progenitor of any transient, the current GW analysis may not be sufficient to identify the ignition process responsible for the transient as seen in Figure 8. Several ignition processes in WD-WD mergers have been suggested: the double detonation in a mass transfer phase like the D^6 model (Guillochon et al. 2010; Fink et al. 2010; Woosley, & Kasen 2011; Pakmor et al. 2013, 2021, 2022; Shen, & Bildsten 2014; Marquardt et al. 2015; Tanikawa et al. 2018, 2019), the car-

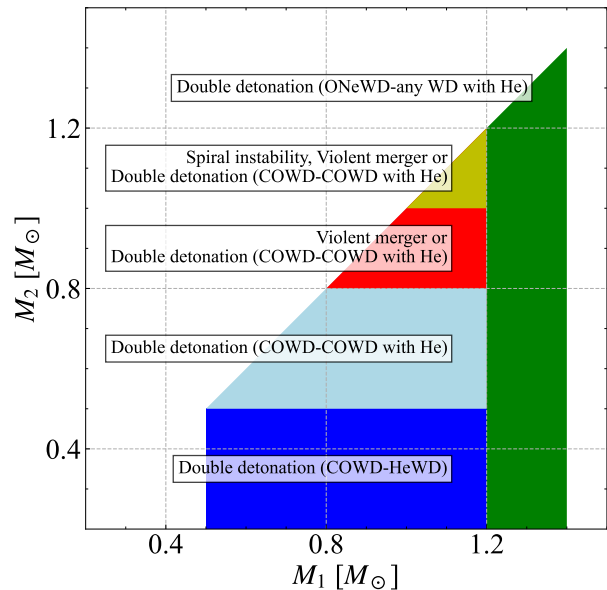


FIG. 8.— Mass combination of WD-WD mergers, and candidates of ignition processes. He and C-O WDs are assumed to have $< 0.5M_{\odot}$ and $0.5\text{--}1.2M_{\odot}$. C-O WDs are allowed to have He shells on their surfaces. The primary WDs are limited to C-O WDs. The double detonation with any WD combinations in DD systems has been suggested by Guillochon et al. (2010); Fink et al. (2010); Woosley, & Kasen (2011); Pakmor et al. (2013, 2021, 2022); Shen, & Bildsten (2014), and Tanikawa et al. (2018, 2019). The (carbon-ignited) violent merger is numerically demonstrated by Pakmor et al. (2010, 2012) and Tanikawa et al. (2015). The spiral instability is reported by Kashyap et al. (2015, 2017). Double detonation in a DD system with an ONe WD can also occur according to Marquardt et al. (2015).

bon detonation in a merger phase like the violent merger model (Pakmor et al. 2010, 2012; Tanikawa et al. 2015), and the carbon detonation via spiral instability in an early and asymmetric accretion disk phase (Kashyap et al. 2015, 2017). If the lighter WD has a sufficiently small mass (say $\lesssim 0.8M_{\odot}$), we can reject the violent merger and spiral instability, as both models need massive secondary WDs, $\gtrsim 0.8M_{\odot}$ and $\gtrsim 1.0M_{\odot}$, respectively (Sato et al. 2016; Kashyap et al. 2017, respectively). If the heavier WD has a sufficiently large mass (say $\gtrsim 1.2M_{\odot}$), we can identify the exploding WD as an oxygen-neon (ONe) WD and adopt the model of Marquardt et al. (2015). However, if the secondary WD mass is close to $1.0M_{\odot}$, we cannot reject any ignition processes, because all the ignition processes are possible in such systems. Note that we may support (or reject) the double detonation model, if we confirm the presence (or absence) of He-detonation ashes by means of detailed spectroscopic observations like MUSSES1604D (Jiang et al. 2017) and ZTF18aaqeaq/SN 2018byg (De et al. 2019).

In our subsequent paper (Takeda et al. in prep.), we will analyze WD-WD mergers in more detail, and distinguish GW signals of ignition processes (see Figure 9). The aforementioned ignition processes should have different GW signals, because they cause explosions at different times with respect to the WD-WD merger time (Δt). WDs explode long before their merger or in the mass transfer phase ($\Delta t \lesssim 0$) in the double detonation

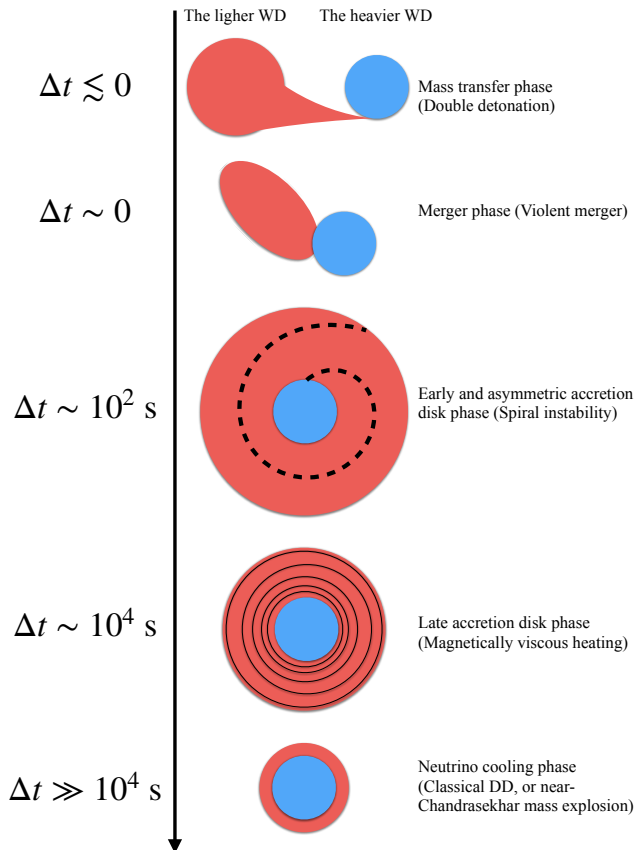


FIG. 9.— Schematic of the relation between ignition processes and WD-WD phases, where Δt is defined as the difference between the ignition time and merger time. Note that, for negative Δt , the merger time would be given if the ignition did not occur. Double detonation can occur before WD-WD mergers. The violent merger initiates at the moment of the merger. Spiral instability can ignite explosive carbon burning at an early and asymmetric accretion disk phase, where the accretion disk is made of the lighter WD tidally disrupted. In a late accretion disk phase, magnetic viscosity heats the system, although there is no scenario for WD explosion in this phase. In a neutrino cooling phase, classical DD scenario (or near-Chandrasekhar mass explosion) may work. The double detonation, violent merger, and spiral instability are studied in references cited in the caption of Figure 8. Dan et al. (2015) investigated WD explosion at a similar phase to the phase of magnetically viscous heating, although they artificially put a hot spot to start carbon detonation. The classical DD was suggested by Webbink (1984) and Iben, & Tutukov (1984).

models, nearly at the moment of their merger ($\Delta t \sim 0$) in the violent merger model, and several 100 seconds after their merger or just after formation of an accretion disk

made from a tidally disrupted WD ($\Delta t \sim 100$ seconds) in the spiral instability model. The signals from GWs just before they disappear due to explosions or mergers may be different among these processes.

Multi-messenger (GW and EM) observations, will be helpful again to specify alternative ignition processes. GW observations can determine the time of disappearance of GW signals with high accuracy. EM observations can give the ignition time with accuracy of ~ 1 hour even in the present day, where the Zwicky Transient Facility archives 2-hour cadence (Bellm 2014), for example. Thus, we can specify ignition processes in which the WD explosion is later than a WD-WD merger by $\gtrsim 1$ hour. If an EM-observed WD explosion happens at 10^4 seconds after a GW-observed WD-WD merger ($\Delta t \sim 10^4$ seconds), magnetically viscous heating in the accretion disk may contribute to the ignition. Note that there is no scenario for WD explosions in this phase to our knowledge. For the case of $\Delta t \gg 10^4$ seconds, we may conclude that the WD explosion occurs along with the classical DD scenario, or near-Chandrasekhar mass explosion through neutrino cooling (e.g. Webbink 1984; Iben, & Tutukov 1984). If that is true, the WD-WD merger remnant experiences slow merging (Yoon et al. 2007), avoiding quasi-static carbon burning, which converts the remnants into oxygen-neon-magnesium WDs (Saio, & Nomoto 1985; Schwab et al. 2016). Even if we do not have any transients, we cannot rule out the possibility of a near-Chandrasekhar mass explosion. The explosion can have a delay time of $\sim 10^5$ yr from the WD-WD merger (Yoon et al. 2007), much more than a human (or civilization) lifespan.

ACKNOWLEDGEMENTS

We would like to greatly thank the anonymous referee for their useful comments to improve our paper. We would like to thank Makoto G. Ando, Takashi Nakamura, Atsushi Nishizawa, Masaki Ando, Kazuhiro Shimasaku, Naoki Seto, Takahiro Sudoh for useful discussion. This work was supported by JSPS KAKENHI Grant No. 17H06360 (AT), 18J00558(TK), 18J21016(HT), 19H00704(HY), 19K03907(AT), and 21K13915(TK). TK acknowledges support from the University of Tokyo Young Excellent Researcher program. HT acknowledge financial support received from the Advanced Leading Graduate Course for Photon Science (ALPS) program at the University of Tokyo. We thank Editage (www.editage.com) for English language editing.

REFERENCES

- Abbott, B. P., Abbott, R., Abbott, T. D., et al. 2016a, *Physical Review Letters*, 116, 061102
- Abbott, B. P., Abbott, R., Abbott, T. D., et al. 2016b, *ApJL*, 818, L22
- Abbott, B. P., Abbott, R., Abbott, T. D., et al. 2017, *Phys. Rev. Lett.*, 119, 161101
- Amaro-Seoane, P., Audley, H., Babak, S., et al. 2017, arXiv e-prints, arXiv:1702.00786
- Amaro-Seoane, P., Andrews, J., Arca Sedda, M., et al. 2022, arXiv:2203.06016
- Arca Sedda, M., Berry, C., Jani, K., et al. 2019, arXiv e-prints, arXiv:1908.11375
- Arun, K. G. 2006, *Phys. Rev. D*, 74, 024025
- Belczynski, K., Holz, D. E., Bulik, T., et al. 2016, *Nature*, 534, 512
- Bellm, E. 2014, in *The Third Hot-wiring the Transient Universe Workshop*, ed. P. R. Wozniak et al. (Santa Fe, NM: Los Alamos National Laboratory), 27
- Berti, E., Buonanno, A., & Will, C. M. 2005, *Phys. Rev. D*, 71, 084025
- Childress, M. J., Wolf, C., & Zahid, H. J. 2014, *MNRAS*, 445, 1898. doi:10.1093/mnras/stu1892
- Cutler, C., & Flanagan, É. E. 1994, *Phys. Rev. D*, 49, 2658
- Cutler, C. 1998, *Phys. Rev. D*, 57, 7089
- Dan, M., Rosswog, S., Guillochon, J., et al. 2011, *ApJ*, 737, 89.

- Dan, M., Guillochon, J., Bruüggen, M., Ramirez-Ruiz, E., & Rosswog, S. 2015, *MNRAS*, 454, 4411
- Damour, T., Iyer, B. R., & Sathyaprakash, B. S. 2001, *Phys. Rev. D*, 63, 044023. doi:10.1103/PhysRevD.63.044023
- Damour, T., Iyer, B. R., & Sathyaprakash, B. S. 2002, *Phys. Rev. D*, 66, 027502. doi:10.1103/PhysRevD.66.027502
- De, K., Kasliwal, M. M., Polin, A., et al. 2017, *ApJ*, 873, 18
- Fink, M., Röpke, F. K., Hillebrandt, W., et al. 2010, *A&A*, 514, A53. doi:10.1051/0004-6361/200913892
- Finn, L. S. 1992, *Phys. Rev. D*, 46, 5236
- Graur, O., Bianco, F. B., & Modjaz, M. 2015, *MNRAS*, 450, 905
- Guillochon, J., Dan, M., Ramirez-Ruiz, E., Rosswog, S. 2010, *ApJ*, 709, L64
- Hachisu, I., Kato, M., & Nomoto, K. 1996, *ApJ*, 470, L97
- Hoeflich, P., Khokhlov, A., Wheeler, C., Phillips, M. M., & Suntzeff, N. B. 1996, *ApJL*, 472, L81
- Iben, I., & Tutukov, A. V. 1984, *ApJS*, 54, 335
- Jha, S. W., Maguire, K., & Sullivan, M. 2019, *Nature Astronomy*, 3, 706
- Jiang, J.-A., Doi, M., Maeda, K., et al. 2017, *Nature*, 550, 80
- Karachentsev, I. D., Makarov, D. I., & Kaisina, E. I. 2013, *AJ*, 145, 101
- Kasen, D., & Woosley, S. E. 2009, *ApJ*, 703, 2205
- Kashi, A. & Soker, N. 2011, *MNRAS*, 417, 1466
- Kashyap, R., Fisher, R., Garcia-Berro, E., et al. 2015, *ApJ*, 800, L7
- Kashyap, R., Fisher, R., Garcia-Berro, E., et al. 2017, *ApJ*, 840, 16
- Koester, D., & Chanmugam, G. 1990, *Reports on Progress in Physics*, 53, 837
- Khan, S., Husa, S., Hannam, M., et al. 2016, *Phys. Rev. D*, 93, 044007
- Kinugawa, T., Inayoshi, K., Hotokezaka, K., Nakauchi, D., & Nakamura, T. 2014, *MNRAS*, 442, 2963
- Kinugawa, T., Miyamoto, A., Kanda, N., & Nakamura, T. 2016, *MNRAS*, 456, 1093
- Kinugawa T., Nakamura T., Nakano H., 2020, *MNRAS*, 498, 3946.
- Kopparapu, R. K., Hanna, C., Kalogera, V., et al. 2008, *ApJ*, 675, 1459
- Kremer, K., Breivik, K., Larson, S. L., et al. 2017, *ApJ*, 846, 95. doi:10.3847/1538-4357/aa8557
- Kuns, K. A., Yu, H., Chen, Y., et al. 2019, arXiv e-prints, arXiv:1908.06004
- Li, W., Chornock, R., Leaman, J., et al. 2011, *MNRAS*, 412, 1473
- Livne, E. 1990 *ApJL*, 354, L53
- Maeda, K., Mazzali, P., Deng, J., et al. 2003, *ApJ*, 593, 22
- Magano, D. M. N., Vilas Boas, J. M. A., & Martins, C. J. A. P. 2017, *Phys. Rev. D*, 96, 083012
- Maggiore, M., *Gravitational Waves* (Oxford University Press, 2007).
- Mandel, I., Sesana, A., & Vecchio, A. 2018, *Classical and Quantum Gravity*, 35, 054004
- Maoz, D., Hallakoun, N., & Badenes, C. 2018, *MNRAS*, 476, 2584. doi:10.1093/mnras/sty339
- Marquardt, K. S., et al. 2015, *A&A*, 580, 118
- McCully, C., Jha, S. W., Foley, R. J., et al. 2014, *Nature*, 512, 54
- McNeill, L. O., Mardling, R. A., & Müller, B. 2020, *MNRAS*, 491, 3000. doi:10.1093/mnras/stz3215
- Moore, C. J., Cole, R. H., & Berry, C. P. L. 2015, *Classical and Quantum Gravity*, 32, 015014. doi:10.1088/0264-9381/32/1/015014
- Nakamura, T., Ando, M., Kinugawa, T., et al. 2016, *Progress of Theoretical and Experimental Physics*, 2016, 093E01
- Ni, W.-T., Wang, G., & Wu, A.-M. 2019, arXiv e-prints, arXiv:1909.04995
- Nishizawa, A., Taruya, A., Hayama, K., et al. 2009, *Phys. Rev. D*, 79, 082002. doi:10.1103/PhysRevD.79.082002
- Nomoto, K. 1982, *ApJ*, 253, 798
- Nomoto, K. 1982, *ApJ*, 257, 780
- Nugent, P., Baron, E., Branch, D., Fisher, A., & Hauschildt, P. H. 1997, *ApJ*, 485, 812
- Pakmor, R., et al. 2022, arXiv:2203.14990
- Pakmor, R., Kromer, M., Röpke, F. K., et al. 2010, *Nature*, 463, 61
- Pakmor, R., Kromer, M., Taubenberger, S., et al. 2012, *ApJ*, 747, L10
- Pakmor, R., Kromer, M., Taubenberger, S., Springel, V. 2013, *ApJ*, 770, L8
- Pakmor, R., Zenati, Y., Perets, H. B., & Toonen, S. 2021, *MNRAS*, 503, 4734
- Perets, H. B., Gal-Yam, A., Mazzali, P. A., et al. 2010, *Nature*, 465, 322
- Phillips, M. M. 1993, *ApJ*, 413, 105
- Romano, J. D. & Cornish, N. J. 2017, *Living Reviews in Relativity*, 20, 2. doi:10.1007/s41114-017-0004-1
- Ruiter, A. J. 2020, *IAU Symposium*, 357, 1, doi: 10.1017/S1743921320000587
- Ruiter, A. J., Belczynski, K., Benacquista, M., et al. 2010, *ApJ*, 717, 1006
- Ruiter, A. J., et al. 2013, *MNRAS*, 425, 36
- Saio, H., & Nomoto, K. 1985, *A&A*, 150, L21
- Santamaria, L., Ohme, F., Ajith, P., et al. 2010, *Phys. Rev. D*, 82, 064016. doi:10.1103/PhysRevD.82.064016
- Sato, Y., Nakasato, N., Tanikawa, A., et al. 2015, *ApJ*, 807, 105
- Sato, Y., Nakasato, N., Tanikawa, A., et al. 2016, *ApJ*, 821, 67
- Seto, N., Kawamura, S., & Nakamura, T. 2001, *Phys. Rev. Lett.*, 87, 221103
- Schwab, J., Quataert, E., Kasen, & D. 2016, *MNRAS*, 463, 3461
- Shen, K. J., & Bildsten, L. 2014, *ApJ*, 785, 61
- Shen, K. J., Kasen, D., Miles, B. J., et al. 2018, *ApJ*, 854, 52
- Shen, K. J., Boubert, D., Gänsicke, B. T., et al. 2018, *ApJ*, 865, 15
- Sullivan, M., Le Borgne, D., Pritchett, C. J., et al. 2006, *ApJ*, 648, 868
- Takeda H., Nishizawa A., Nagano K., Michimura Y., Komori K., Ando M., Hayama K., 2019, *PhRvD*, 100, 042001. doi:10.1103/PhysRevD.100.042001
- Tanikawa, A., Nakasato, N., Sato, Y., et al. 2015, *ApJ*, 807, 40
- Tanikawa, A., Nomoto, K., & Nakasato, N. 2018, *ApJ*, 868, 90
- Tanikawa, A., Nomoto, K., Nakasato, N. & Maeda, K. 2019, *ApJ*, 885, 103
- Tanikawa A., Yoshida T., Kinugawa T., Trani A. A., Hosokawa T., Susa H., Omukai K., 2022, *ApJ*, 926, 83.
- Totani, T., Morokuma, T., Oda, T., et al. 2008, *PASJ*, 60, 1327
- Taubenberger, S. 2017, in *Handbook of Supernovae*, ed. A. W. Alsabti & P. Murdin (Cham: Springer), 317
- van den Broek, D., Nelemans, G., Dan, M., et al. 2012, *MNRAS*, 425, L24
- Webbink, R. F. 1984, *ApJ*, 277, 355
- Whelan, J., & Iben, I. 1973, *ApJ*, 186, 1007
- Willems, B., Kalogera, V., Vecchio, A., et al. 2007, *ApJ*, 665, L59
- Wolz A., Yagi K., Anderson N., Taylor A. J., 2021, *MNRAS*, 500, L52. doi:10.1093/mnras/slz183
- Woosley, S. E., & Kasen, D. 2011, *ApJ*, 734, 38
- Woosley, S. E., Taam, R. E., & Weaver, T. A. 1986, *ApJ*, 301, 601
- Yamanaka, M., Maeda, K., Tanaka, M., et al. 2016, *PASJ*, 68, 68
- Yoon, S.-C., Podsiadlowski, P., & Rosswog, S. 2007, *MNRAS*, 380, 933